

Surface-enhanced Raman scattering for magnetic semiconductor ZnSe:Fe hybrid structures

A. R. de Moraes, E. Silveira,* D. H. Mosca, N. Mattoso, and W. H. Schreiner

Departamento de Física—UFPR, Centro Politécnico, Caixa Postal 19044, 81531-990 Curitiba-PR, Brazil

(Received 27 November 2001; revised manuscript received 11 March 2002; published 7 May 2002)

Micro-Raman spectroscopy has been carried out on hybrid systems consisting of magnetic Fe and Co nanoclusters immersed in a semiconductor ZnSe host. The experimental results clearly reveal surface-enhanced Raman scattering for the ZnSe matrix phonon modes. The intensity enhancement correlates with the Fe content and sample morphology. Enhancement factors of up to about one order were achieved, as compared to the pure ZnSe sample.

DOI: 10.1103/PhysRevB.65.172418

PACS number(s): 75.50.Pp, 78.30.Fs, 78.30.Er

One of the novel approaches of creating new electronic devices is based on the control of not only the charge, but also the spin of electrons.^{1,2} In the so-called spintronics field, the study of hybrid semiconductor ferromagnetic structures is attracting more and more attention.^{3–5} Most of the work done up till now on diluted magnetic semiconductors or composite structures used samples fabricated by molecular-beam epitaxy. Alternative efforts using much cheaper and simpler electrodeposition methods recently succeeded in fabricating such hybrid systems.⁶

Hybrid systems combining ZnSe and Fe have been pointed out as attractive candidates to be explored, since they have modest lattice mismatch and high chemical stability at the Fe/ZnSe interfaces. In addition ZnSe is one of the most promising II–VI materials for optoelectronic applications due to its direct band gap in the blue-green region of the visible spectrum.

Raman scattering is a very powerful and versatile tool for the characterization of new materials. For more than 20 years⁷ it has been known that the proximity of metallic structures to a sample has profound effects on the Raman spectra of that sample. The selection rules as well as the mode intensities can be altered by the presence of the metal.⁸ The Raman spectra of certain molecules adsorbed on specially prepared metal surfaces are even a 10^6 -fold more intense than expected, due to the so-called surface-enhanced Raman scattering (SERS). It has been recognized that the enhancement has both a chemical and an electromagnetic origin.⁹ Since its discovery, SERS has been demonstrated with many molecules and with a number of metals, including Cu, Ag, Au, Li, Na, K, In, Pt, and Rh. Very recently SERS from bare Fe electrodes was observed for the first time. Depending critically on the Fe surface roughening procedure, surface-enhancement factors of two to three orders for pyridine adsorbed on Fe were achieved.¹⁰ Despite the fact that SERS spectroscopy has been successfully used to study molecules adsorbed on rough metal surfaces, only a few attempts succeeded in observing this effect for semiconductor systems on metals. Honma *et al.*¹¹ have observed SERS of CdS from Ag-CdS hybrid colloidal particles in solution and Suh and Lee¹² reported for the first time SERS of CdS nanowires grown on predeposited Ag into anodic aluminum oxide pores. On the other hand, the observed intensity enhancements in the Raman spectra of semiconductors are nor-

mally related to resonance phenomena, i.e., when the incident laser resonates with a strong interband electronic transition.¹³

In this work we report on micro-Raman spectroscopy carried out on hybrid systems consisting of magnetic Fe and Co nanoclusters immersed in a semiconductor ZnSe host. The experimental results clearly reveal an increase in the scattered intensities of the ZnSe matrix phonon modes, that correlates with the Fe content and sample morphology. Enhancement factors of up to about one order were achieved for samples electrochemically grown from plating solutions with the highest Fe concentration. This finding opens up a range of interesting new possibilities for optical studies of such hybrid systems, including, e.g., (i) interactions between photogenerated carriers and phonons of the semiconductor matrix and (ii) the electromagnetic coupling between the metal clusters. Both phenomena should have influence on the transport and magnetic properties. Other Raman measurements were performed in order to investigate the desorption of a Se excess in the outermost layer from a ZnSe:Co sample. The high laser intensity used for the measurement was able to cause the desorption of Se prompting us to investigate the Raman spectra on line and *in situ*. All the samples were grown on mechanically and chemically polished stainless-steel substrates by simultaneous electrochemical deposition of Zn, Se, and Fe or Co. Aqueous solutions containing reagent grade ZnSO₄, SeO₂, and Fe(NH₄)₂(SO₄)₂ or CoSO₄ were used as electrolyte solutions with different molar concentrations. The micrometer-thick films were electrodeposited at 65 °C under potentiostatic conditions using a conventional stationary parallel-plate system. More details about the growth procedure and the electrochemical conditions can be found elsewhere.⁶ As shown in our previous work, ferromagnetic clusters with a multidomain structure dominate the magnetic properties of these samples.¹⁴

The Raman-scattering measurements were performed at room temperature in the backscattering configuration from the sample growth surface. The 514.5-nm line (2.41 eV) of an Ar⁺ laser was focused to a spot diameter of about 2 μm. After being dispersed by a Jobin-Yvon T64000 micro-Raman system, the scattered light was detected by a liquid nitrogen-cooled charge coupled device. The spectral resolution was set to about 4 cm⁻¹.

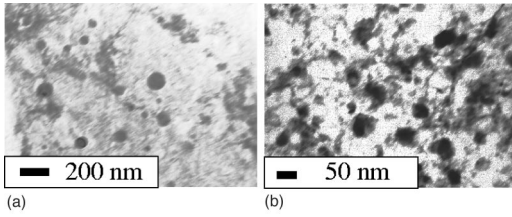


FIG. 1. TEM bright field micrographs of ZnSe:Fe samples prepared from solutions containing (a) 1/8 mM Fe and (b) 1 mM Fe.

Figure 1 shows transmission electron microscopy (TEM) bright field images from two ZnSe:Fe samples, obtained using a JEOL 1200EX-II electron microscope. A typical image of a sample prepared from the solution containing 1/8 mM Fe is shown in Fig. 1(a). Fe clusters (dark regions), exhibiting an almost physically uncoupled network, are dispersed in the ZnSe matrix. They have an average size of about 95 nm. A typical image of the sample obtained from the solution with 1 mM Fe is shown in Fig. 1(b). Here again, mainly due to the high electronic density difference, it is possible to distinguish Fe-rich regions (dark zones). Below the percolation threshold the clustering process is a segregation-nucleation diffusion and growth process. Although the sample shows similar average size for the Fe clusters, one can observe an increase in the cluster density, and consequently a larger interaction between them. For higher concentrations the samples exhibit percolating regions, having average sizes as large as 950 nm.

Figure 2 depicts the Raman spectra of four ZnSe:Fe electrodeposited samples grown under different conditions. An increase of Fe incorporation in the samples going from (a) to (d) is expected, with (a) being a pure ZnSe sample. The spectra were shifted vertically for better visualization. The range between 180 cm^{-1} and 320 cm^{-1} of each spectra of Fig. 2 was fitted using three Lorentzian line shapes, in order to obtain the frequency position, the linewidth and the integrated intensity of each peak. These fitting parameters are given in Table I. For all the spectra shown in Fig. 2 one can observe a structure at 252 cm^{-1} , attributed to the LO phonon of the ZnSe matrix, and a weak leakage from the TO as a shoulder at 205 cm^{-1} . Both modes are expected for pure crystalline ZnSe.¹⁵ The pronounced peak at about 235 cm^{-1} can be attributed to a trigonal Se phase,^{16,17} since an excess of Se on top of a stoichiometric ZnSe template naturally occurs due to the growth conditions. We will address this issue later. The second-order zone-boundary $2TA(X)$ mode at about 140 cm^{-1} can be more clearly observed for the samples labeled as (a) and (b). Increasing Fe content causes the spectra range under 150 cm^{-1} to become more pronounced, indicating an increase of disorder in the samples, since these modes are known to be disorder activated. Figure 2 exhibits a pronounced increase in the scattered intensity for the ZnSe LO and TO phonons with increasing Fe content. An equivalent increase of the second-order ZnSe LO mode intensity can also be observed at about 500 cm^{-1} . Similarly to small area electron diffraction (SAED) pattern and x-ray diffraction,¹⁴ Raman measurements showed no evidence of

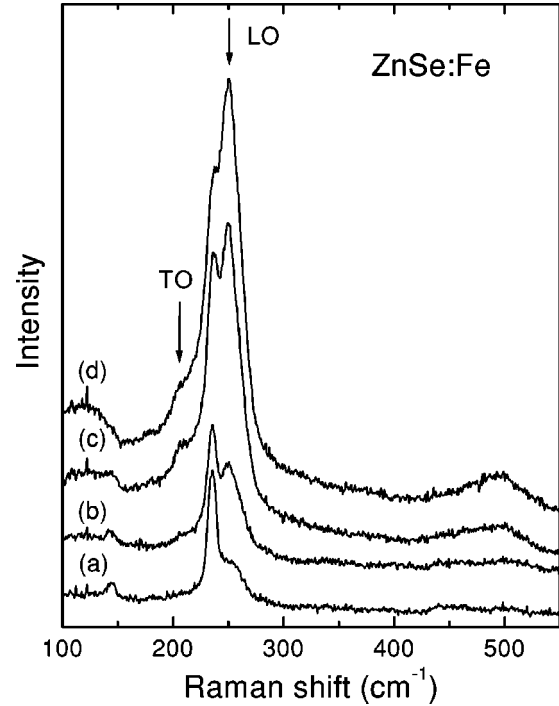


FIG. 2. Room-temperature Raman spectra of (a) pure ZnSe deposited at -0.85 V . (b), (c), and (d) correspond to ZnSe:Fe samples deposited under periodically pulsed potentials between -0.85 V and -1.1 V for, respectively, (b) 1 s and 0.1 s from 1 mM Fe solution; (c) 1 s and 0.1 s from 100 mM Fe solution and (d) 1 s and 1 s from 100 mM Fe solution.

intermediate compounds. Thus, no change in the gap of the material is expected and consequently resonance effects can be excluded. We attribute the spectral enhancement in our samples to the surface-enhanced Raman scattering of ZnSe due to the formation of Fe granules inside the sample. This effect is mainly due to the resonant excitation of surface plasmons on the Fe clusters, rather than to chemisorption. In fact, as the ZnSe TO-LO peak positions and widths remain practically unchanged for all the samples, as shown in Table I, no intermediate compound of the $\text{Zn}_{1-x}\text{Fe}_x\text{Se}$ type is expected to be present in our samples.¹⁵ Besides the fact that the chemical effect represents a change in the nature and identity of the adsorbed material, its magnitude rarely exceeds a factor of 10^{-5} in comparison with the electromagnetic effect.⁹ Previous SERS studies have shown that a pres-

TABLE I. Fitting parameters for the frequency position ω in cm^{-1} , full width at half maximum Γ in cm^{-1} and integrated intensity I in arbitrary units for the peaks between 180 cm^{-1} and 320 cm^{-1} shown in the Raman spectra of Fig. 2.

Spectrum	ZnSe-LO	ZnSe-TO	Se
	$\omega(\Gamma;I)$	$\omega(\Gamma;I)$	$\omega(\Gamma;I)$
(a)	253 (21; 9)	205 (25; 2)	236 (9; 14)
(b)	252 (22; 21)	204 (25; 6)	235 (12; 14)
(c)	252 (21; 62)	205 (25; 19)	236 (15; 30)
(d)	252 (22; 88)	205 (25; 22)	235 (18; 39)

ence of some kind of surface roughness is a necessary, although not sufficient, requirement for a great surface-enhancement factor.^{9,10} An increase of Fe incorporation and consequently interface area and roughness is expected in the samples going from (a) to (d), as shown by TEM analysis above. The Raman peaks integrated intensity, shown in Table I allowed for the enhancement factors to be obtained. An enhancement factor of about one order of magnitude for the ZnSe-LO mode was achieved for the sample labeled as (d), i.e., obtained from plating solutions with the highest Fe concentration, in comparison with the pure ZnSe sample. In fact, SERS intensities were found to increase rapidly with decreasing interparticle separation, due to coupling effects.¹⁸ Linss *et al.*¹⁹ succeeded to find a correlation between linear optical constants and Raman enhancement in phthalocyanine thin solid films with incorporated silver clusters. Assuming nonabsorbing phthalocyanine molecules and a uniform distribution of cluster sizes, a simple semiclassical estimation of the enhancement factor could be provided. In our case, the cluster size distribution is not uniform at all. Besides, the electrodynamic interaction between the clusters may cause an extra complication in the optical behavior of the sample, specially for the samples with high Fe content, which exhibits even percolating regions. The accurate prediction of the optical behavior of this type of sample and its relation to SERS effect is complicated from a theoretical point of view and it is beyond the scope of this work.

Although the Raman spectra of the ZnSe:Co samples are very similar to the ZnSe:Fe samples no SERS effect could be observed. One of the possible reasons is the difference in the average cluster sizes of both samples and consequently in the film morphology. Such correlation has been demonstrated for SERS from molecules adsorbed on Ag spheres of different sizes and shapes.⁹ In our case plating solutions with 1/4 mM Fe, for example, gives origin to Fe clusters having average sizes of about 95 nm with clear boundaries and rounded shapes. On the other hand, for plating solutions with 1/4 mM Co, the Co clusters exhibit less clear boundaries and an average size of about 250 nm.¹⁴

Let us turn now to the analysis of the phonon peak at 235 cm^{-1} , previously ascribed to a trigonal Se phase mode.^{16,17} A Raman spectrum taken from the substrate showed no modes in this range. The assignment of the 235- cm^{-1} peak to the trigonal phase is in agreement with previous x-ray Photoemission Spectroscopy profile analyses, which showed an excess of Se near the surface of our samples. Also X-ray diffraction analysis could not rule out the trigonal Se phase formation.²⁰ The Se-rich outermost layer can act in our samples as a natural protection layer against contamination of the ZnSe surface during exposure to air. Analogous procedures are carried out for GaAs or even ZnSe MBE grown layers using As and Se capping, respectively.^{17,21} Raman spectra taken from a ZnSe:Co sample, grown from a plating solution containing 50 mM Co, for different times during the laser cap-removal process are shown in Fig. 3. The spectra are shifted vertically for the sake of clarity. Although the contribution of Se seems to be much prominent in the ZnSe:Fe samples, we decided to use only the ZnSe:Co samples in the laser cap-removal

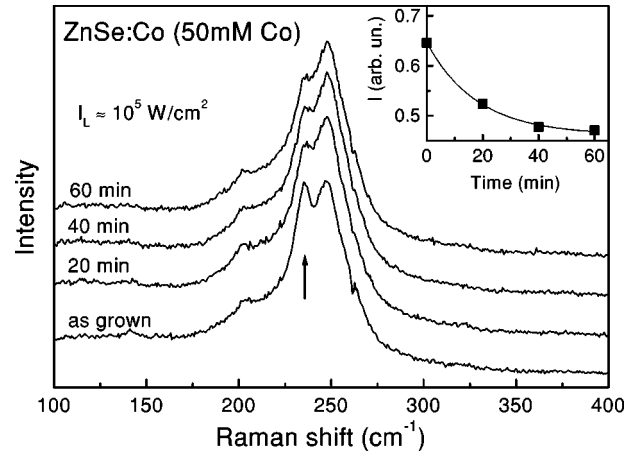


FIG. 3. Room-temperature Raman spectra of the ZnSe:Co sample grown from a 50 mM Co solution. The black arrow indicates the phonon mode attributed to an excess Se phase. The inset shows the dependence of the Se mode intensity as a function of the exposure time to the intense laser beam.

experiment in order to avoid contributions from SERS effect on the integrated intensities of the Raman peaks. Indicated by the black arrow are the peaks related to the Se trigonal phase. While the ZnSe TO and LO modes, at 205 cm^{-1} and 252 cm^{-1} respectively, maintain their positions and full widths at half maximum, the intensity of the Se mode at 235 cm^{-1} decreases as a function of exposure time to the incident laser. In the inset of Fig. 3 the integrated intensity of the Se trigonal peak is plotted against the exposure time of sample to the incident laser beam. The dependence of the Se peak intensity on laser exposure time shows an exponential decay behavior, as revealed by the solid curve. As the intensity of the incident laser beam is about 10^5 W/cm^2 , and consequently large compared to previous measurements, we attribute the intensity decay as a laser-based removal of the Se layer from the sample surface. It is also worth to note that from the data in Table I the enhancement factor for the ZnSe LO peak at the ZnSe:Fe samples is about one order of magnitude, while the enhancement factor for the Se trigonal peak is only about 3 going from spectrum (a) to (d), therefore, the SERS effect comes predominantly from the granular structure of the Fe clusters in bulk.

In conclusion, we have measured the surface enhanced Raman scattering from ZnSe:Fe hybrid structures without need of specially prepared SERS substrates. Our results clearly reveal an increase in the ZnSe matrix phonon modes scattered intensities that correlates with the Fe content and sample morphology. These findings reveal possibilities of study and control of optical processes and electromagnetic coupling in hybrid structures.

The authors are indebted to CME-UFPR and GPO-UNICAMP for technical help with the experiments. This work was partially supported by CNPq, PROCAD-CAPES, PRONEX/MCT and FUNPAR (Brazilian funding agencies).

*Electronic address: edilson@fisica.ufpr.br

- ¹H. Ohno, *Science* **291**, 840 (2001), and references therein.
- ²G. A. Prinz, *J. Magn. Magn. Mater.* **200**, 57 (1999).
- ³Y. D. Park, A. Wilson, A. T. Hanbicki, J. E. Mattson, T. Ambrose, G. Spanos, and B. T. Jonker, *Appl. Phys. Lett.* **78**, 2739 (2001).
- ⁴S. Haneda, H. Munekata, Y. Takatami, and S. Koshihara, *J. Appl. Phys.* **87**, 6445 (2000).
- ⁵P. J. Wellmann, J. M. Garcia, J.-L. Feng, and P. M. Petroff, *Appl. Phys. Lett.* **73**, 3291 (1998).
- ⁶A. R. de Moraes, D. H. Mosca, N. Mattoso, and W. H. Schreiner, *Electrochem. Solid-State Lett.* **5**, C11 (2002), a more detailed description of the periodically pulsed potential electrodeposition is currently in preparation and will be published separately.
- ⁷M. Fleischmann, P. S. Hendra, and A. S. McQuillan, *Chem. Phys. Lett.* **26**, 123 (1974).
- ⁸E. J. Ayars, H. D. Hallen, and C. L. Jahncke, *Phys. Rev. Lett.* **85**, 4180 (2000).
- ⁹For a review see Martin Moskovits, *Rev. Mod. Phys.* **57**, 783 (1985).
- ¹⁰P. G. Cao, J. L. Yao, B. Ren, B. W. Mao, R. A. Gu, and Z. Q. Tian, *Chem. Phys. Lett.* **316**, 1 (2000).
- ¹¹I. Honma, T. Sano, and H. Komiyama, *J. Phys. Chem.* **97**, 6692 (1993).
- ¹²J. S. Suh and J. S. Lee, *Chem. Phys. Lett.* **281**, 384 (1997).
- ¹³*Light Scattering in Solids I-VIII*, edited by M. Cardona and G. Güntherodt (Springer, Berlin, 1975).
- ¹⁴A. R. de Moraes, D. H. Mosca, N. Mattoso, E. Silveira, W. H. Schreiner, and A. J. A. de Oliveira (unpublished).
- ¹⁵C.-L. Mak, R. Sooryakumar, B. T. Jonker, and G. A. Prinz, *Phys. Rev. B* **45**, 3344 (1992).
- ¹⁶V. V. Poborchii, A. V. Kolobov, and K. Tanaka, *Appl. Phys. Lett.* **72**, 1167 (1998).
- ¹⁷D. Drews, A. Schneider, D. R. T. Zahn, D. Wolfframm, and D. A. Evans, *Appl. Surf. Sci.* **104/105**, 485 (1996).
- ¹⁸L. Gunnarsson, E. J. Bjerneld, H. Xu, S. Petronis, B. Kaseno, and M. Käll, *Appl. Phys. Lett.* **78**, 802 (2001).
- ¹⁹V. Linns, O. Stenzel, and D. R. T. Zahn, *J. Raman Spectrosc.* **30**, 531 (1999).
- ²⁰A. R. de Moraes, D. H. Mosca, W. H. Schreiner, N. Mattoso, and E. Silveira, *Braz. J. Phys.* (to be published).
- ²¹U. Resch, N. Esser, Y. S. Raptis, W. Richter, J. Wasserfall, A. Förster, and D. I. Westwood, *Surf. Sci.* **269/270**, 797 (1992).